Assessment of Irrigation Water Distribution Using Remotely Sensed Indicators: A Case Study of Doho Rice Irrigation Scheme, Uganda

Article · August 2023

DOI: 10.1016/j.atech.2023.100184

Fawaz Wamala
Makerere University

Anthony Gidudu
Makerere University

Prossie Nakawuka
Washington State University

Erion Bwambale
Makerere University

Smart Agricultural Technology 4 (2023) 100184

Contents lists available at ScienceDirect

Smart Agricultural Technology

journal homepage: www.journals.elsevier.com/smart-agricultural-technology

Assessment of irrigation water distribution using remotely sensed indicators: A case study of Doho Rice Irrigation Scheme, Uganda

Fawaz Wamala [a], Anthony Gidudu [a], Joshua Wanyama [b], Prossie Nakawuka [b], Erion Bwambale [b,*], Abebe D. Chukalla [c]

[a] Department of Geomatics and Land Management, Makerere University, P. O. Box 7062, Kampala, Uganda
[b] Department of Agricultural and Biosystems Engineering, Makerere University, P. O. Box 7062, Kampala, Uganda
[c] The Department of Land and Water Management, IHE Delft Institute for Water Education, 2611 AX 6 Delft, the Netherlands

ARTICLE INFO

Edited by Editor: S.K.

Keywords:
Actual evapotranspiration
Irrigation performance assessment
Surface energy balance system
Equity
Adequacy

ABSTRACT

The rising competition for scarce land and water resources and the need to satisfy the global food demand from an ever-growing population necessitates novel methods to monitor irrigation scheme performance for improved water use efficiency. The traditional methods employed in sub-Saharan Africa to assess irrigation performance are point-based, expensive, and time-consuming, making monitoring and evaluation of these capital-intensive projects difficult. This study aimed at employing satellite data with high spatial and temporal resolution in assessing the performance of Doho Rice Irrigation Scheme through estimations of actual evapotranspiration. Actual evapotranspiration (ET_a) was modelled from Landsat 7 imagery using the surface energy balance system algorithm on five clear days between January and April 2020. Using equity and adequacy metrics, the derived ET_a was used to assess the irrigation performance of the scheme. Results showed that the equity indicator was generally fair, with the coefficient of variation between 0.11 and 0.08, close to the 0.10 threshold implying irrigation water is fairly distributed within the scheme. The average adequacy was 0.87, above the 0.65 threshold, indicating adequate water supply throughout the scheme. The study's findings can be used in future research and benchmarking with other irrigation schemes to address the country's water resource management challenges.

1. Introduction

The projected global population growth and the expected increase in food demand coupled with the changing climate patterns are likely to constrain water use for agricultural production [1–3]. In addition, irrigated agriculture has shaped itself at the centre of meeting the future food demand amidst climate change and sustainability challenges [4]. As much as 70% of the world's freshwater is abstracted for irrigation purposes, a significant portion of it is lost due to inefficient irrigation systems [5]. Therefore, performance assessment in irrigated agriculture is a requirement for sustainable food production. The performance level of surface and pressurized irrigation systems and their sustainability will determine if humanity will be able to meet the food demand by 2050 amidst climate change challenges [6].

In sub-Saharan Africa, assessing the performance of irrigation systems has been carried out by various scholars [1, 7-11]. However, one common challenge reported by these scholars is insufficient data in conducting the studies. Most irrigation schemes have poor record-keeping systems and also lack water accounting infrastructure, thus hindering primary data collection for research. This is usually attributed to the high cost associated with monitoring, lack of measurement structures and poor scheme management. This has affected the modernization plans of most schemes as baseline data is insufficient. Coupling ground-based observations and remotely sensed data would help the surface irrigation scheme in sub-Saharan Africa curb this problem.

Remote sensing is a powerful tool that can be used to understand agricultural performance at high spatial and temporal resolutions [12–14]. The application of remote sensing in estimating agricultural performance indicators is becoming more prolific as it provides more information, in both time and space than can be provided by traditional methods, such as water balance or ground measurements [15, 16]. Remote sensing can provide insight into various aspects of agricultural production, including the estimation of ET_a and biomass production

* Corresponding author.
E-mail address: erion.bwambale@mak.ac.ug (E. Bwambale).

https://doi.org/10.1016/j.atech.2023.100184
Received 25 May 2022; Received in revised form 9 January 2023; Accepted 10 January 2023
Available online 19 January 2023

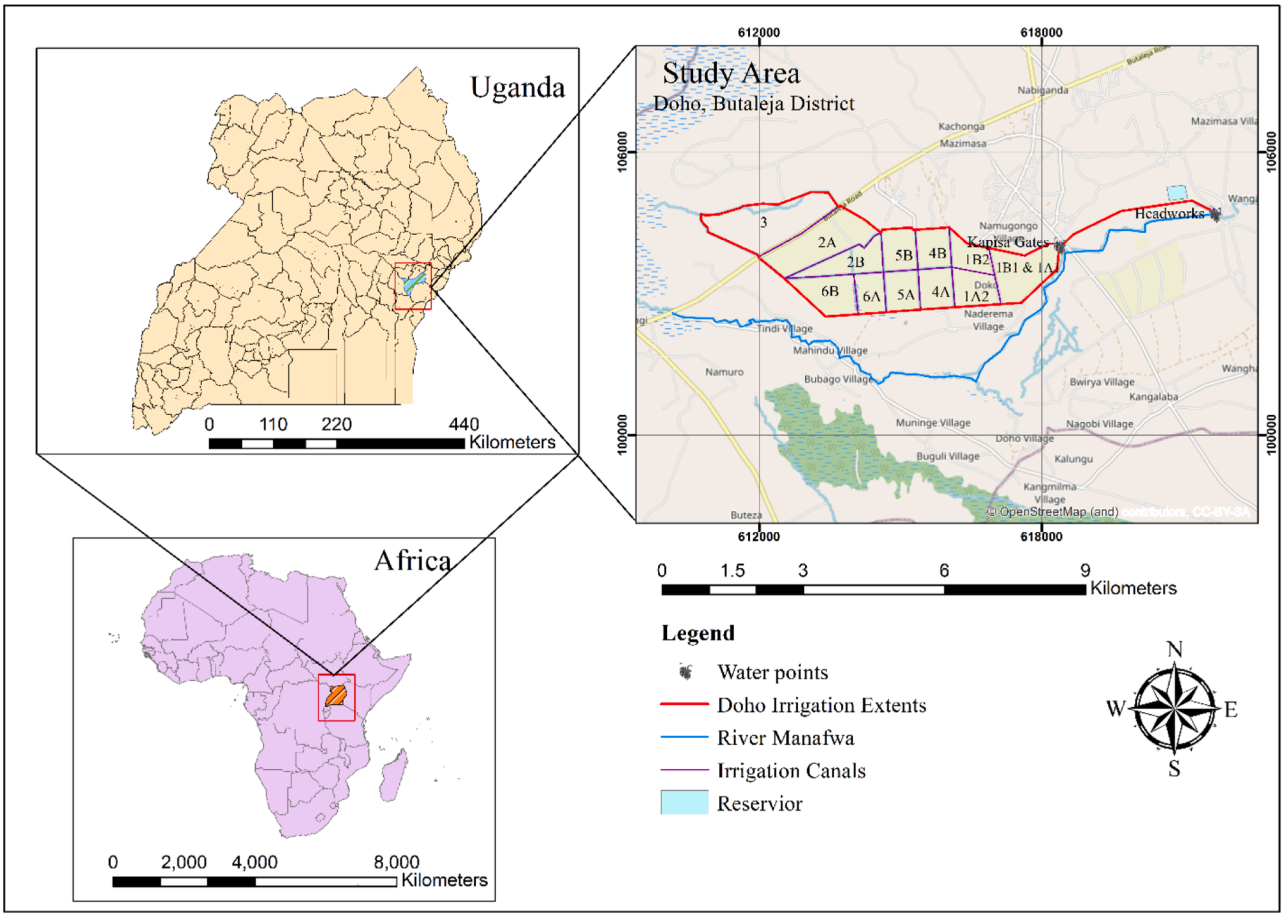

Fig. 1. Location of Doho Rice Irrigation Scheme.

[17]. With the increase in open access to satellite imagery and retrieval algorithms, remote sensing provides effective yet spatially and temporally extensive options to estimate agricultural indices, especially for evaluating irrigation performance in data-scarce regions, like Africa [17]. The use of remote sensing to estimate and evaluate various indicators for irrigation performance at the irrigation scheme level (i.e., the irrigation perimeter) has been tested and reported for multiple spatial and temporal resolutions.

Several authors have used remote sensing to assess the performance of irrigated agriculture across Africa's surface irrigation schemes [13, 18-22]. However, no such study has been conducted in Ugandan irrigation schemes and as a result, little is known about the data-scarce irrigated agricultural systems in the country. Remote sensing presents an opportunity for data-scarce regions to carry out scheme to basin-wide analysis to assess irrigated agriculture performance.

Doho Rice Irrigation Scheme located in Butaleja District, Uganda faces major challenges, including poor water distribution, deteriorating irrigation systems, silting canals and lack of water measuring systems [23, 24]. The traditional methods currently used to assess irrigation performance in Uganda are point-based measurements that take time to collect the necessary data, rendering it expensive in the long run. The purpose of this study was to assess the performance of irrigation water distribution at Doho Rice Irrigation Scheme using remotely-sensed indicators in order to determine spatial-temporal changes in irrigation delivery at the scheme. Satellite imagery were acquired from Land Sat 7 at the USGS website during the rice growing season from January to April 2020

Table 1
Salient features of the studied irrigation schemes.

System Name	Doho Rice Irrigation Scheme
Type of system	River diversion
Name of river	River Manafwa
Management system	Government/Cooperative Society
Command area (ha)	1000
Scale *	Large
Land holding within the scheme**	Smallholder
Average size of farm area (ha) per household	0.2
Number of households	3927
Cropping pattern	Lowland rice
Cropping intensity (%)	200
Average Annual rainfall, P (mm)	1186
Annual potential evaporation, ET_o (mm)	1617

2. Materials and methods

2.1. Description of the study area

Doho Rice Irrigation Scheme which commenced production in 1942 is situated in the northern bank of the Manafwa River at 34°03′ East of the Greenwich and 0° 56′ North of the Equator in both the Mazimasa and Kachonga Sub-Counties of East Bunyole County in Uganda's Butaleja District, as shown in Fig. 1. It has 2500 hectares, of which 2380 have been cultivated with rice and the remaining 120 hectares cover scheme infrastructure such as agricultural roads, reservoirs, water transmission lines and bridges [23]. The scheme is sub-divided into 11 key blocks, namely, 1A, 1B, 2A, 2B,3, 4A, 4B, 5A, 5B, 6A, and 6B, through which water is distributed via drawn up schedules depending on water

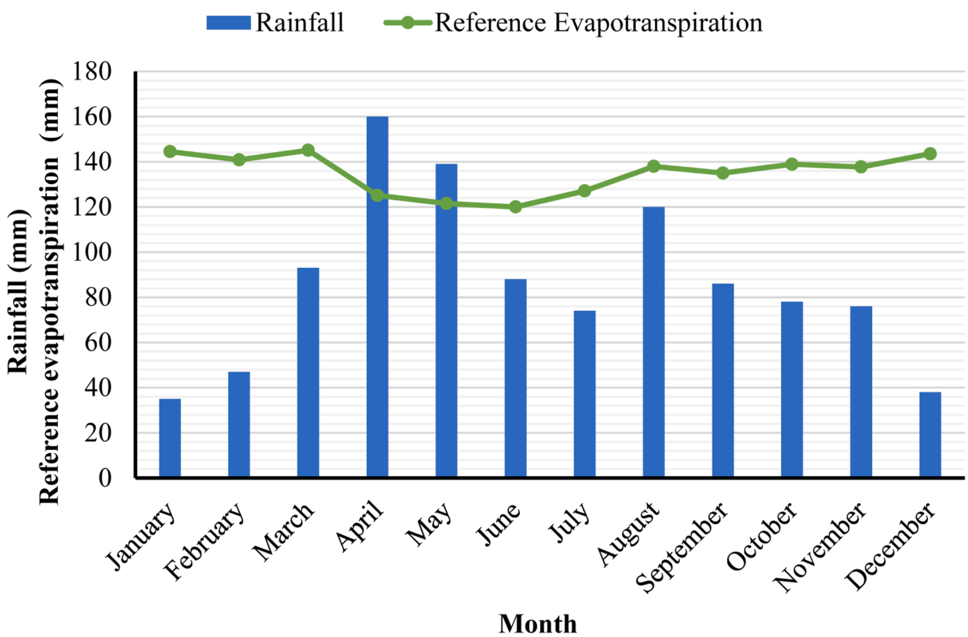

Fig. 2. Monthly variation of rainfall and reference evapotranspiration.

available in River Manafwa. Detailed characteristics of the scheme are presented in Table 1.

2.2. Remote sensing data

Landsat 7 ETM+ data sets with a full aperture, 5 percent absolute radiometric calibration, a Thermal infrared (TIR) signal of 60-metre spatial resolution, and a revisit time of 16 days was used in this study. This data was freely available via the USGS Earth Explorer data portal (https://earthexplorer.usgs.gov/). Landsat 7 is the calibrated and reliable Earth-observing satellite ever put into orbit. Furthermore, since the research area is contained inside a single scene (Path 170 Row 059), it was possible to download at least two images per month and focus solely on the cloud-free available from January to April 2020. Landsat 7 was chosen over Landsat 8 because of its spatial resolution of thermal band 6. Every image has a spatial resolution of 60 m and 6 bands (Bands 1–5 and 7) covering visible and near-infrared (NIR) wavelengths. In addition, a thermal band (Band 6) is also included in the images, recorded at 60-metre spatial resolution and was resampled to 30 metre spatial resolution using the nearest neighbour method.

2.3. Meteorological data

Meteorological data was obtained from the National Aeronautics and Space Administration (NASA) Earth data portal through the Global Land Data Assimilation System (GLDAS). GLDAS is a one-of-a-kind uncoupled land surface modelling system that runs many models and incorporates a vast amount of observed data, to ingest satellite and ground-based observed values. It runs on a global scale with a spatial resolution of 0.25° and 3 h of step data [25]. Therefore, when working with places where data is scarce or there is no ground meteorological information, using GLDAS datasets is very beneficial [26, 27]. The NASA Giovanni Earth Data portal provides air temperature data, air pressure, specific air humidity, wind speed, longwave and shortwave radiation (https://giovanni.gsfc.nasa.gov/giovanni/) was obtained monthly for the study area. The data was also resampled using the nearest neighbour approach to match the 30 m spatial resolution of the satellite images. Fig. 2 shows the monthly variation of rainfall and reference evapotranspiration at Doho Rice Irrigation Scheme.

2.4. Surface energy balance model for ET_a

The SEBS model, a residual method was utilized in this study since it is available in Integrated Land and Water Information System (ILWIS), open-source software that is simple to use, unlike other models that require much experience to build or apply in commercial software. The input data layers, such as surface albedo, Normalized Difference Vegetation Index (NDVI), surface emissivity, and land surface temperature, required to run the SEBS model, were created using satellite images and meteorological inputs for the appropriate acquisition period.

Surface Albedo is the average reflectance of the sun's spectrum with values ranging from 0 to 1 basing on the land cover. It is calculated using a statistical relationship established from radiative transfer simulations as expressed in Eq. (1) [28].

$$\alpha = \frac{0.356B_1 + 0.130B_3 + 0.373B_4 + 0.085B_5 + 0.072B_7 - 0.0018}{1.016} \quad (1)$$

Where B stands for satellite bands.

NDVI helps differentiate bare soil from grass, detect plants under stress, and differentiates between crops and their growth stages [29]. It is expressed as:

$$NDVI = \frac{NIR - Red}{NIR + Red} \quad (2)$$

Surface emissivity refers to the surface ability to transform heat energy into radiant energy. It is widely expressed using a logarithmic expression based on NDVI as expressed in Eq. (3) [30].

$$\varepsilon = 1.0094 + 0.047\ In(NDVI) \quad (3)$$

In the residual method, latent heat (λET_a) is calculated as a residual of the surface energy budget using the above inputs applying the SEBS expression in Eq. (4).

$$ET_a = (R_n - H - G)/\lambda \quad (4)$$

where λETa is the turbulent latent heat flux (λ is the latent heat of vaporization), R_n is the net radiation, H is the turbulent sensible heat flux, and G is the soil heat flux. However, satellite images represent an instantaneous observation in time and hence ET_a was in initially mm s^{-1}. Daily evapotranspiration was therefore determined based on the evaporative fraction, assumed to remain constant throughout the day

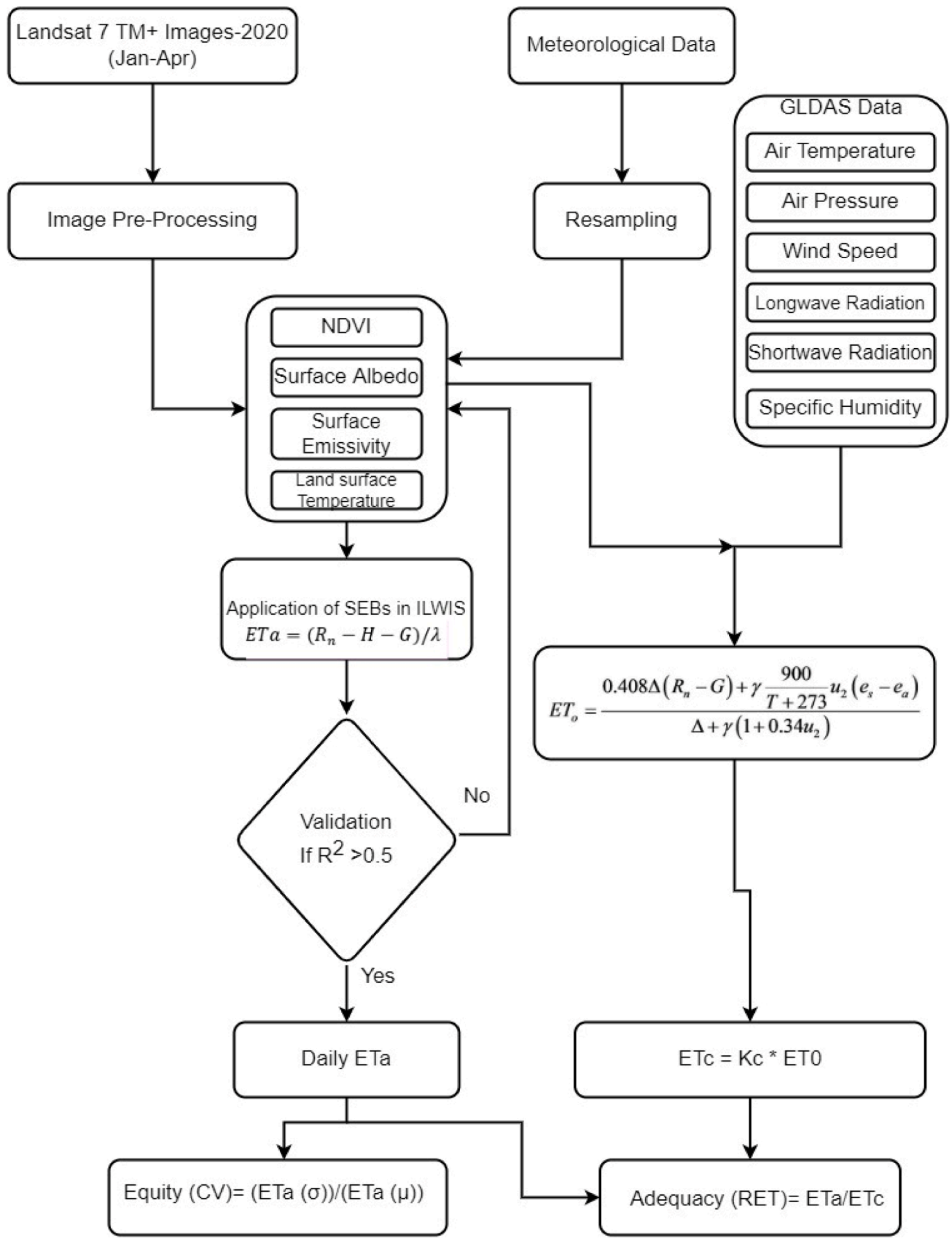

Fig. 3. Summary of the methodology. Adapted from ([35]).

[31]. Total daily evapotranspiration was determined following Eq. (7) in [32]:

The equation to calculate the net radiation is given by:

$$R_n = (1 - \alpha) * R_{swd} + \varepsilon * R_{lwd} - \varepsilon * \sigma * T_s^4 \tag{5}$$

where α is the surface albedo, R_{swd} is the downward solar radiation, R_{lwd} is the downward longwave radiation, ε is the surface emissivity, σ is the Stefan-Boltzmann constant, and T_s is the surface temperature.

The soil heat flux equation is parameterized as:

$$G = \frac{T}{\alpha}\left(0.0038\alpha + 0.007\alpha^2\right)\left(1 - 0.98NDVI^4\right)R_n \tag{6}$$

When calculating turbulent sensible heat flux, Eq. (7) is used.

$$H = \rho_{air} * C_P * \frac{T_{aero} - T_a}{r_r} \tag{7}$$

where T_{aero} is the ‘aerodynamic surface temperature’ obtained by extrapolating the logarithmic air temperature profile to the roughness length for heat transport or, more precisely, to the sum of the zero-plane displacement height [33]; r_r is a radiometric-convective resistance.

2.5. Validation of ET_a using the advection-aridity (AA) – in situ model

The AA model was used for the validation of ET_a derived using the SEBS algorithm. In the absence of direct measurement of ET_a in the field, Brutsaert & Stricker [34] proposed the AA method to calculate ET_a using only a few in situ meteorological parameters which are easily and routinely available at standard weather stations. Scientists have widely used this method to validate remotely sensed ET_a, especially in data-scarce areas [32, 35, 36]. The method is largely empirical, and it is derived from an adaptation and integration of ideas suggested previously in the literature [37–39]. It progresses to just a unique and quick parametric equation that is simple to apply [34]. The AA model for estimating sectoral evapotranspiration expresses the ET_a as a blend of the wet environment (ET_W) and potential evapotranspiration.

$$ET_a = 2ET_w - ET_O \tag{8}$$

where ET_a is the actual evapotranspiration, ET_w is the evapotranspiration under a wet surface, and ET_0 is the potential evapotranspiration [35].

For wet surface evapotranspiration, Priestley & Taylor (P-T) equation [34, 40]:

$$ET_w = \alpha_e \frac{\Delta}{\Delta + \gamma}(R_N - G) \tag{9}$$

The sole recommended way to determine ET_O is to use the FAO Penman-Monteith method. This method is employed because short crop ET_O is directly related and explicitly covers physiological and aerodynamic properties at the studied location. Considering all this, Eq. (10) by [41] was employed to calculate ET_O:

$$ET_0 = \frac{\Delta}{\Delta + \gamma}(R_N - G) + \frac{\gamma}{\Delta + \gamma} * E_r \tag{10}$$

And an empirical wind function $f(u_2)$ for determination of relative evaporation E_r as:

$$E_r = f(u_2) * (e_{sat} - e_a) \tag{11}$$

where $(R_N - G)$is the net available energy at the surface, $\alpha_e = 1.26$ is the Priestley & Taylor (P-T) coefficient, Δ is the slope of saturated water vapour pressure gradient at the current air temperature ($kPa\ ^\circ C^{-1}$), γ is the psychometric constant ($kPa\ ^\circ C^{-1}$), $f(u_2)$ is estimated in the form of $f(u_2) = 0.26(1 + 0.54u_2)$, $u_2$is the mean wind speed (ms^{-1}) at a given height above the ground surface, while e_a and e_{sat} are the actual and saturation vapour pressures, respectively [35].

The AA model is a point method that uses in situ meteorological data from the nearest weather stations to the study area for the time of the research. Data used for this model included temperature, humidity, and wind speed. This data was acquired from both the Doho Irrigation Scheme weather station and the Tororo weather station.

2.6. Estimation of crop evapotranspiration, ET_c

ET_c is a term that refers to the maximum amount of ET required by a certain crop type with specific attributes under complete soil water supply, but not necessarily a saturated surface, as ET_0 does [42]. Under the same climatic conditions, differences in leaf anatomy, stomatal features, aerodynamic qualities, and even albedo lead the ET_c to differ from the ET_O. ET_c was calculated using Eq. (12) as discussed by [43].

$$ET_c = K_c * ET_O \tag{12}$$

Where K_c is the crop coefficient linear segment model proposed by the FAO specifications and varying at each crop stage. Given that rice growers dominate the irrigation scheme under study, the K_c values for rice were used. ET_O is the reference evapotranspiration mmday^{-1}

2.7. Irrigation water distribution indicators

2.7.1. Equity

This is a critical element of irrigation management, which deals with the spatial distribution of water from the perspective of the system manager for large supply-based irrigation systems [44]. Equity does not implicate equality and to differentiate the two, statistical measures of deviation from the mean ought to be used [45]. Akhtar et al. [35] used the Coefficient of Variation (CV) of ET_a to estimate the equity of an irrigation system at sub-basin level.

$$Equity\ (CV) = \frac{Standard\ deviation\ of\ ETa\ (\sigma)}{Mean\ of\ ETa\ (\mu)} \tag{13}$$

If an irrigation scheme is supply-based rather than demand-based, there would be a thin layer of an equal amount of water to various subunits [46]. Therefore, a low CV of ET_a across the irrigation system would indicate low inequity and vice versa.

Table 2
ET_aAA and ET_{aSEBS} estimates in mm d^{-1} over station-1.

Date	ET_{aSEBS}	ET_{aAA}	Error ($ET_{aSEBS} - ET_{aAA}$)	Absolute Error
09/01/2020	1.867	1.642	0.228	0.228
25/01/2020	1.834	1.917	−0.083	0.083
10/02/2020	1.847	2.249	−0.403	0.403
13/03/2020	1.878	0.749	1.128	1.128
30/04/2020	1.831	2.318	−0.488	0.488
			MAE	0.466
			R^2	0.709
			RMSE	0.588

Table 3
ET_{aAA} and ET_{aSEBS} estimates in mm d^{-1} over station-2.

Date	ET_{aSEBS}	ET_{aAA}	Error ($ET_{aSEBS} - ET_{aAA}$)	Absolute Error
09/01/2020	1.918	1.799	0.118	0.118
25/01/2020	1.878	2.062	−0.184	0.184
10/02/2020	1.835	2.283	−0.448	0.448
13/03/2020	1.932	1.015	0.917	0.917
30/04/2020	1.896	2.054	−0.158	0.158
			MAE	0.365
			R^2	0.682
			RMSE	0.472

2.7.2. Adequacy

The adequacy indicator is used to measure the sufficiency of water delivery to a known command area as well as the reduction in ET_a [47]. Bos et al. [45] stresses that all indicators that measure adequacy must include an estimation of demand. The demand may be strictly scientific, such as ET demand for specific crops, or it can include soil water requirements, such as those used to estimate land preparation water requirements and water lost through natural seepage and percolation. Akhtar et al. [35] employed the relative ET to detect water shortages in a given time frame. The following dimensionless ratio can be used to give valuable information to the water manager:

$$Adequacy\ (RET) = \frac{ET_a}{ET_c} \tag{14}$$

According to Bandara [48], RET=0.65 is the critical value of this indicator, and anything below that is considered a poor irrigation system performance, which gradually leads to a loss of crop yield and biomass. Additionally, higher RET values in a scheme indicate that it is under less stress, and vice versa [49]. RET of 0.75 to 1.0 indicates sufficient water supply [46]. The flow chart provided in Fig. 3 sums up all the steps followed in executing the methodology.

3. Results and discussion

3.1. Validation of SEBS-estimated ET_a with AA model estimates

Actual evapotranspiration estimations from SEBS (ET_{aSEBS}) were compared to in-situ actual evapotranspiration from the advection aridity equation (ET_{aAA}). Table 2 and Table 3 shows ET_{aAA} and ET_{aSEBS} in mm d^{-1} estimations over stations 1 and 2, respectively, for the 5 days investigated in this research. An error analysis of SEBS evapotranspiration relative to Advection Aridity evapotranspiration was also performed, with errors defined by subtracting ETa_{AA} from ETa_{SEBS}. The mean absolute errors (MAE) for both stations were relatively low, indicating few overestimations during the five days of the study.

Based on these validation results, the ET_a estimated by SEBS and the ET_a calculated by AA at the two meteorological stations have a good fit, with coefficients of determination $R^2 = 0.71$ and $R^2 = 0.68$, respectively.

Table 4
SEBS computed ET_a maximum, minimum, mean, and standard deviation in mmday^{-1}.

Date	Max	Min	Mean	Standard deviation
09/01/2020	2.20	0.00	1.87	0.16
25/01/2020	2.19	0.00	1.86	0.13
10/02/2020	2.13	0.00	1.83	0.12
13/03/2020	1.95	0.00	1.87	0.13
30/04/2020	2.10	0.00	1.82	0.13

The highest ET_a estimated by AA was 2.32 mmday-1 in a dry month, with a lowest of 0.749 mmday-1 realized in a chilly month. These findings are consistent with those of [35], who found that in cool months, the AA model estimations were lower than the SEBS estimates. This was ascribed to the fact that the AA model employs a version of the Penman-Monteith equation which does not perform well during periods when the available energy (R_n) is negative or extremely near to zero.

3.2. Spatial distribution of actual evapotranspiration

Using the SEBS algorithm in ILWIS software, the actual evapotranspiration of Doho Rice Irrigation Scheme was calculated for all cloud-free days throughout the study period. Table 4 shows the fundamental statistical characteristics of the calculated ET_a in the scheme across the 5 days of this research.

The maximum computed ET_a throughout the catchment area ranged from 1.95 to 2.20 mmday^{-1} as shown in Table 4. The mean actual evapotranspiration ranged from 1.82 to 1.87 mmday^{-1}, indicating that estimated values were clustered towards the mean and showed minimal variation. This variability in SEBS predicted values is similar to that reported by Rwasoka et al. [32] when estimating ET_a in Zimbabwe's Upper Manyame catchment.

Figs. 4 (a-e) shows the SEBS modelled spatial distribution of actual evapotranspiration in the scheme across the study period.

The values registered per day represent the amount of water lost from a cropped surface in millimeters of water depth. A case in point, a value of 2.19mmday^{-1} recorded on January 25, 2020 indicates that 21.9 m^3 of water per hectare were lost from the cropped surface. This also

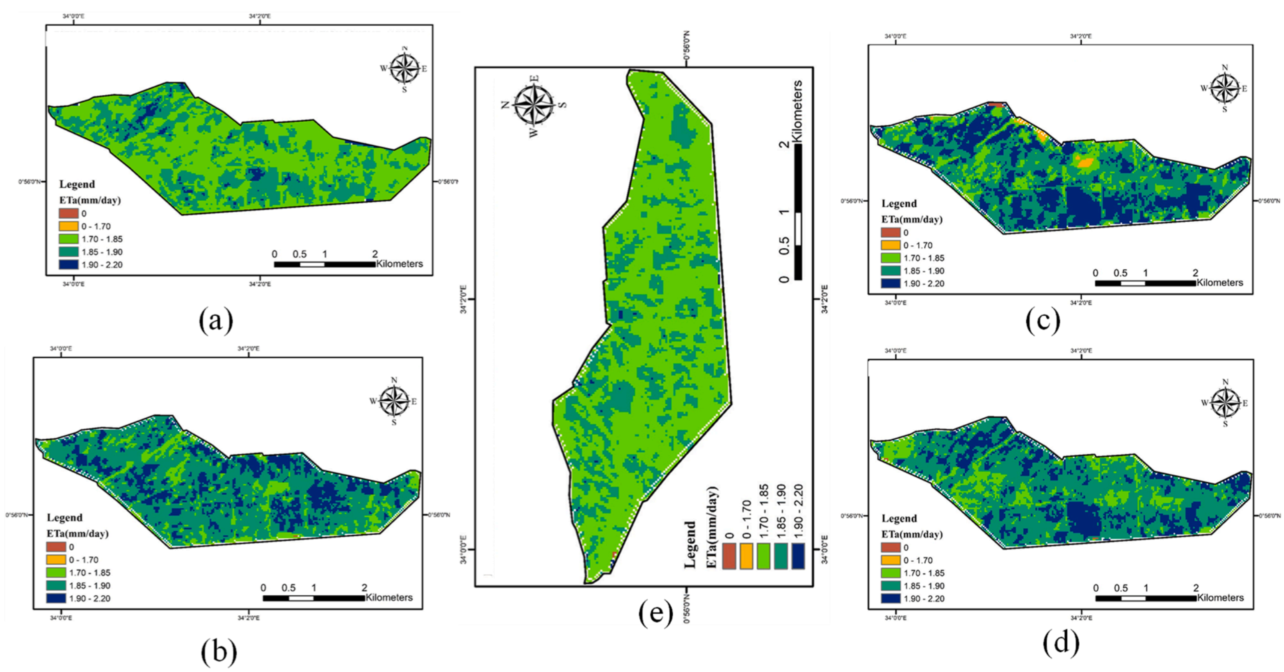

Fig. 4. SEBS modelled spatial distribution of actual evapotranspiration in the scheme across the study period. (a)-(e) estimated ET_a by SEBS on 09/01/2020, 25/01/2020, 10/02/2020, 13/03/2020, 30/04/2020.

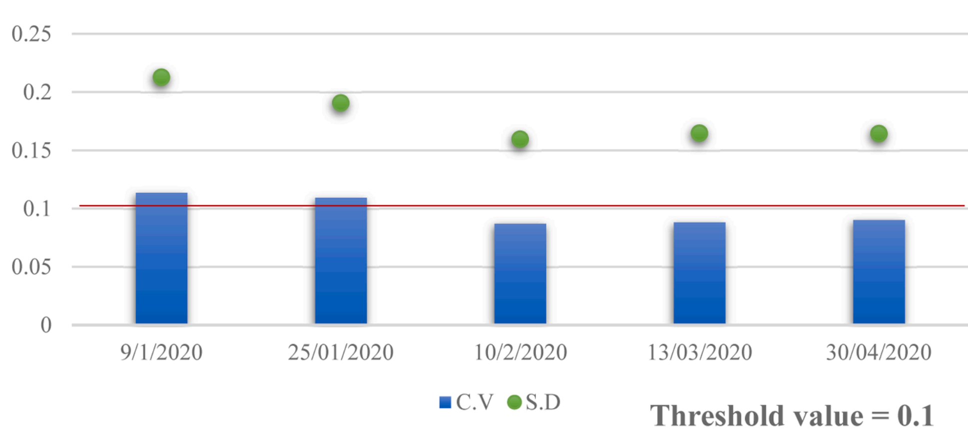

Fig. 5. Spatial equity of water for the days studied.

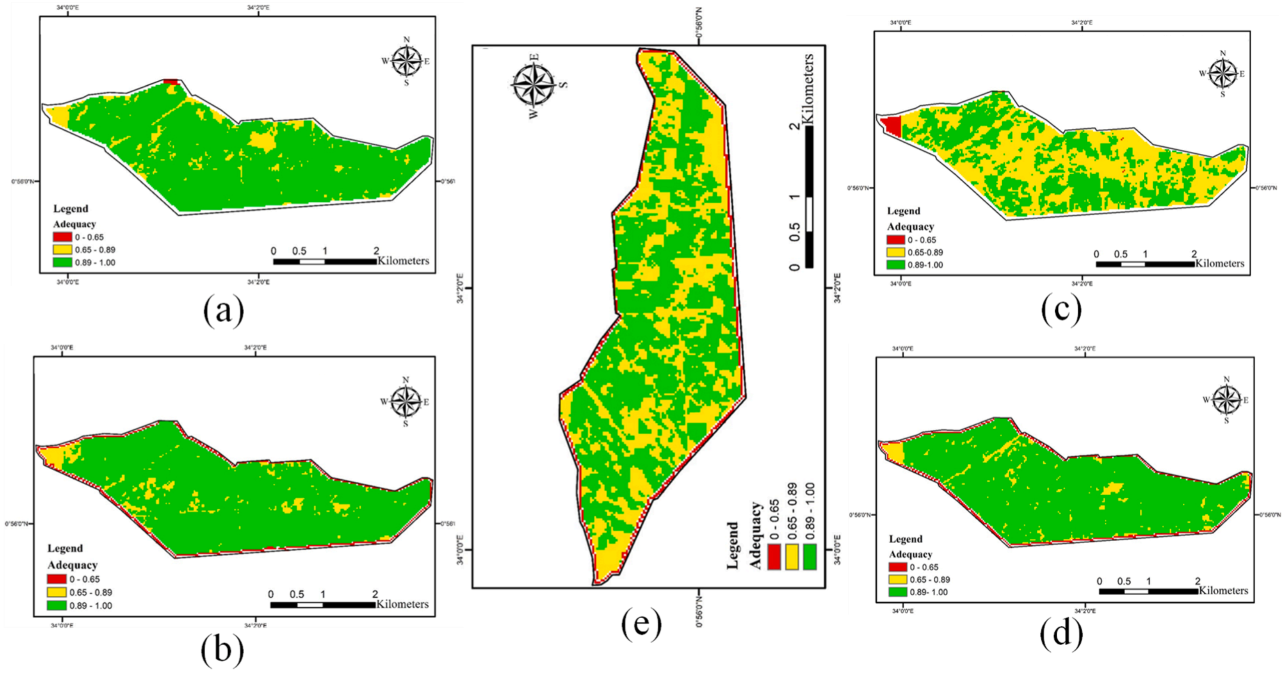

Fig. 6. Spatial-temporal variation of adequacy (a)-(e) registered on 09/01/2020, 25/01/2020, 10/02/2020, 13/03/2020, 30/04/2020 respectively.

shows that a lot of water was lost from the fields in January, as it had higher values than the other months studied. This is due to the high temperatures that accompany the month of January. Because April is a wet month, low ET_a values were recorded on 30/04/2020, indicating that less water was lost per hectare from the cropped surface.

These results also show that the areas with the highest estimated actual evapotranspiration in the Doho Irrigation scheme were in the southern sections of blocks 5A and 4A and the north-eastern parts of blocks 1B1 and 1A1 near the Kapisa gates, where water is fed into the scheme. Estimated ET_a in these places was roughly in the upper 80% of the range of estimated values on a specific day. This is owing to the high quantity of water and low elevation in these blocks. On the other hand, Fig. 4(a)-(e) clearly show that the scheme's northwest and some parts of the southwest experienced lower ET_a rates, with values in the lower 20% of the predicted ET_a range.

3.3. Irrigation performance assessment

3.3.1. Equity

Spatial Equity is a crucial characteristic to consider when evaluating the performance of an irrigation scheme using the coefficient of variation (CV). The equity indicator is tested against a criterion where 0.00–0.10 and a standard deviation (S.D) less than 10% is considered good, 0.11–0.25 is considered acceptable, and greater than 0.25 is considered poor. Fig. 5 displays the CV and corresponding S.D of Doho Rice Irrigation Scheme for each day studied.

These results reveal that spatial equity was typically fair and acceptable during the study period, with the best result ($\sigma = 15.9\%$, CV $= 0.08$) reported on the 10/February/2020 and the worst result ($\sigma = 21.3\%$, CV $= 0.11$) registered on the 10/January/2020, a hot day. These findings are similar to those obtained by [23] while conducting a hydraulic performance evaluation of the Doho Rice Irrigation Scheme's water conveyance system.

A further analysis was done on individual blocks of the scheme with results displayed in the Appendix A. These revealed that field blocks 1B1 and 1A1 performed poorly (high inequity) on all of the days studied, with no day scoring above the threshold values. This is typically linked to the fact that the Doho Rice Irrigation Scheme is supply-based rather than demand-based, resulting in a thin layer of identical quantity of water being provided to different blocks regardless of the cropping pattern.

3.3.2. Adequacy

Figs. 6(a)-(e) show the results of the Doho Rice Irrigation Scheme's sufficiency for water use measured using the adequacy indicator for the study period investigated. The mean value for spatial adequacy was 0.87 throughout the study period, which was higher than the essential threshold of 0.65 and indicates a fair sufficient water supply throughout the scheme.

The results show that there is high inadequacy in both February and April, implying that crop water requirements were substantially more than the water delivered by the water managers. As a result, supply was not carried out in accordance with crop water requirements throughout these months. These results are similar to those acquired by Akhtar et al. [35] while measuring irrigation performance in large river basins under data-scarce conditions in the Kabul River basin, Afghanistan, where they obtained an average adequacy value of 0.84 over their study's summer period.

4. Conclusions

The method used to estimate ET_a and the results obtained from this study could potentially be used in future research and benchmarking with other irrigation schemes, which will play an important role in the country's investment plans tackling water resource management challenges.

Irrigation managers should develop a water distribution schedule informed by objective data from field blocks for better spatial distribution results or embrace digital irrigation operation systems such as installing canals equipped with modules and combined with automatic or fixed regulators. Since such modern facilities have been tested and programmed to meet equity irrigation goals, the spatial variability across the scheme will be reduced.

Irrigation managers should conduct regular surveys to examine water-stressed areas of the scheme. To aid this, pertinent institutions should invest proactively in the improvement and modernization of

Table A1
Equity of water supplied for the month of 09/January/2020.

Field Block Name	Mean	Standard deviation	Spatial Coefficient of Variation (CV)	Comment
3	1.867	0.216	0.116	Acceptable
2A	1.867	0.085	0.045	Good
2B	1.882	0.034	0.018	Good
6B	1.894	0.029	0.015	Good
6A	1.908	0.033	0.017	Good
5B	1.845	0.077	0.041	Good
5A	1.924	0.084	0.043	Good
4B	1.869	0.039	0.020	Good
4A	1.904	0.037	0.019	Good
1B2	1.876	0.026	0.014	Good
1A2	1.892	0.033	0.017	Good
1B1 & 1A1	1.877	0.171	0.091	Acceptable
Overall Scheme	**1.874**	**0.213**	**0.114**	**Acceptable**

Table A2
Equity of water supplied for the month of 25/January/2020.

Field Block Name	Mean	Standard deviation	Spatial Coefficient of Variation (CV)	Comment
3	1.875	0.112	0.059	Acceptable
2A	1.872	0.051	0.027	Good
2B	1.873	0.025	0.013	Good
6B	1.879	0.022	0.011	Good
6A	1.883	0.025	0.013	Good
5B	1.873	0.020	0.011	Good
5A	1.895	0.167	0.088	Acceptable
4B	1.862	0.019	0.010	Good
4A	1.879	0.031	0.016	Good
1B2	1.871	0.025	0.013	Good
1A2	1.881	0.025	0.013	Good
1B1 & 1A1	1.871	0.168	0.090	Acceptable
Overall Scheme	**1.869**	**0.191**	**0.109**	**Acceptable**

irrigation infrastructure by implementing cutting-edge technologies such as Remote Sensing to guide water managers on when, where, and how much water to distribute. This can also be accomplished by building the capacity of local labour and shifting the system from a supply-based to a demand-based one to attain water sufficiency.

Author contributions

All authors have read and agreed to publish the manuscript.

CRediT authorship contribution statement

Fawaz Wamala: Conceptualization, Formal analysis, Investigation, Visualization, Methodology. **Anthony Gidudu:** Supervision, Project administration, Writing – review & editing. **Joshua Wanyama:** Project administration, Resources, Supervision. **Prossie Nakawuka:** Visualization, Writing – review & editing. **Erion Bwambale:** Methodology, Conceptualization, Supervision, Writing – original draft, Writing – review & editing. **Abebe D. Chukalla:** Writing – original draft, Writing – review & editing.

Declaration of Competing Interest

The authors declare that they have no known competing financial interests or personal relationships that could have appeared to influence the work reported in this paper.

Data availability

Data will be made available on request.

Table A3
Equity of water supplied for the month of 10/February/2020.

Field Block Name	Mean	Standard deviation	Spatial Coefficient of Variation (CV)	Comment
3	1.851	0.074	0.040	Good
2A	1.834	0.028	0.015	Good
2B	1.831	0.032	0.017	Good
6B	1.847	0.029	0.015	Good
6A	1.847	0.029	0.016	Good
5B	1.837	0.031	0.016	Good
5A	1.857	0.077	0.041	Good
4B	1.823	0.033	0.018	Good
4A	1.843	0.036	0.019	Good
1B2	1.834	0.047	0.026	Good
1A2	1.843	0.031	0.017	Good
1B1 & 1A1	0.826	0.165	0.199	Acceptable
Overall Scheme	**1.835**	**0.159**	**0.087**	**Acceptable**

Table A4
Equity of water supplied for the month of 13/March/2020.

Field Block Name	Mean	Standard deviation	Spatial Coefficient of Variation (CV)	Comment
3	1.875	0.074	0.039	Good
2A	1.872	0.052	0.027	Good
2B	1.886	0.025	0.013	Good
6B	1.871	0.021	0.011	Good
6A	1.879	0.021	0.011	Good
5B	1.881	0.026	0.014	Good
5A	1.864	0.074	0.040	Good
4B	1.880	0.031	0.016	Good
4A	1.875	0.129	0.069	Acceptable
1B2	1.897	0.018	0.009	Good
1A2	1.884	0.024	0.013	Good
1B1 & 1A1	1.857	0.167	0.090	Acceptable
Overall Scheme	**1.870**	**0.165**	**0.088**	**Acceptable**

Table A5
Equity of water supplied for the month of 30/April/2020.

Field Block Name	Mean	Standard deviation	Spatial Coefficient of Variation (CV)	Comment
3	1.823	0.110	0.060	Acceptable
2A	1.834	0.054	0.029	Good
2B	1.837	0.025	0.014	Good
6B	1.830	0.023	0.012	Good
6A	1.832	0.026	0.014	Good
5B	1.840	0.025	0.013	Good
5A	1.823	0.080	0.043	Good
4B	1.836	0.026	0.014	Good
4A	1.840	0.028	0.015	Good
1B2	1.818	0.024	0.013	Good
1A2	1.816	0.034	0.018	Good
1B1 & 1A1	1.805	0.164	0.091	Acceptable
Overall Scheme	**1.822**	**0.164**	**0.090**	**Acceptable**

Funding Information

No funding was received for this research.

Acknowledgement

We want to thank the Department of Geomatics and Land Management and the Department of Agricultural and Biosystems Engineering, Makerere University for providing the necessary environment for this study to be conducted. Sincere gratitude goes to the unknown reviewers whose comments improved the quality of the manuscript.

Appendix A

Table A1, Table A2, Table A3, Table A4, Table A5

References

[1] J. Benavides, E. Hernández-Plaza, L. Mateos, E. Fereres, A global analysis of irrigation scheme water supplies in relation to requirements, Agric. Water Manag. 243 (August 2020) (2021), 106457, https://doi.org/10.1016/j.agwat.2020.106457.
[2] D. Gerten, et al., Feeding ten billion people is possible within four terrestrial planetary boundaries, Nat. Sustain. 3 (3) (2020) 200–208, https://doi.org/10.1038/s41893-019-0465-1.
[3] A.V. Pastor, et al., The global nexus of food–trade–water sustaining environmental flows by 2050, Nat. Sustain. 2 (6) (2019) 499–507, https://doi.org/10.1038/s41893-019-0287-1.
[4] E. Bwambale, F.K. Abagale, G.K. Anornu, Smart irrigation monitoring and control strategies for improving water use efficiency in precision agriculture: a review, Agric. Water Manag. 260 (107324) (Feb. 2022) 1–12, https://doi.org/10.1016/j.agwat.2021.107324.
[5] FAO, IFAD, UNICEF, WFP, and WHO, In Brief to The State of Food Security and Nutrition in the World 2021, FAO, IFAD, UNICEF, WFP and WHO, Rome, Italy, 2021.
[6] FAO, The Future of Food and Agriculture: Trends and Challenges, 4, 2017.
[7] J. Hakuzimana, B. Masasi, Performance evaluation of irrigation schemes in Rugeramigozi Marshland, Rwanda, Water Conserv. Manag. 4 (1) (2020) 7–14, https://doi.org/10.26480/wcm.01.2020.07.14.
[8] D. Kambou, et al., Evaluation and proposals for improving irrigation performance around small reservoirs in Burkina Faso, J. Irrig. Drain. Eng. 145 (6) (2019), 05019004, https://doi.org/10.1061/(asce)ir.1943-4774.0001386.
[9] F.M. Muema, P.G. Home, J.M. Raude, application of benchmarking and principal component analysis in measuring performance of public irrigation schemes in Kenya, Agriculture 8 (10) (2018) 162, https://doi.org/10.3390/agriculture8100162.
[10] S. Phiri, T.N. Reuben, G. Chipula, K.A. Wiyo, Evaluation of furrow irrigation performance: case of Kasinthula Cane Growers Scheme in Malawi, African J. Sci. Technol. Innov. Dev. 0 (0) (2021) 1–9, https://doi.org/10.1080/20421338.2021.1889767.
[11] T. Adongo, F. Abagale, G. Kranjac-Berisavljevic, Performance assessment of irrigation schemes in northern Ghana using comparative performance indicators, Int. J. Sci. Eng. Technol. (5) (2016) 217–224.
[12] E. Bwambale, et al., Towards precision irrigation management: a review of GIS, remote sensing and emerging technologies, Cogent Eng 9 (1) (2022) 1–21, https://doi.org/10.1080/23311916.2022.2100573.
[13] M. Blatchford, C.M. Mannaerts, Y. Zeng, H. Nouri, P. Karimi, Influence of spatial resolution on remote sensing-based irrigation performance assessment using WaPOR data, Remote Sens 12 (18) (2020), https://doi.org/10.3390/RS12182949.
[14] M.L. Blatchford, et al., Evaluation of WaPOR V2 evapotranspiration products across Africa, Hydrol. Process. 34 (15) (2020) 3200–3221, https://doi.org/10.1002/hyp.13791.
[15] M.L. Blatchford, C.M. Mannaerts, Y. Zeng, H. Nouri, P. Karimi, Status of accuracy in remotely sensed and in-situ agricultural water productivity estimates: a review, Remote Sens. Environ. 234 (October) (2019), 111413, https://doi.org/10.1016/j.rse.2019.111413.
[16] A.R. Safi, P. Karimi, M. Mul, A. Chukalla, C. de Fraiture, Translating open-source remote sensing data to crop water productivity improvement actions, Agric. Water Manag. 261 (2022), 107373, https://doi.org/10.1016/j.agwat.2021.107373.
[17] A.D. Chukalla, et al., a framework for irrigation performance assessment using WaPOR data: the case of a sugarcane estate in Mozambique, Hydrol. Earth Syst. Sci. Discuss. (September) (2021) 1–26, https://doi.org/10.5194/hess-2021-409.
[18] A. Elnmer, M. Khadr, A. Allam, S. Kanae, A. Tawfik, Assessment of irrigation water performance in the nile delta using remotely sensed data, Water 10 (10) (2018), https://doi.org/10.3390/w10101375.
[19] G. Mostafa, Developing a Mobile GIS Application for Facilitating Information Communications in Agri-Environmental Programs, 2019.
[20] A. Sawadogo, L. Kouadio, F. Traoré, S.J. Zwart, T. Hessels, K.S. Gündoğdu, Spatiotemporal assessment of irrigation performance of the kou valley irrigation scheme in burkina faso using satellite remote sensing-derived indicators, ISPRS Int. J. Geo-Inf. 9 (8) (2020), https://doi.org/10.3390/ijgi9080484.
[21] I. Tantawy, "The application of the FAO WaPOR data portal to monitor efficient water use in agriculture: a case study on the Eastern Nile River Basin," TU DELFT, 2019.
[22] I. Weerasinghe, W. Bastiaanssen, M. Mul, L. Jia, A. Van Griensven, Can we trust remote sensing evapotranspiration products over Africa, Hydrol. Earth Syst. Sci. 24 (3) (2020) 1565–1586, https://doi.org/10.5194/hess-24-1565-2020.
[23] E. Bwambale, P. Home, J. Raude, J. Wanyama, Hydraulic performance evaluation of the water conveyance system of Doho Rice Irrigation Scheme in Uganda, J. Sustain. Res. Eng. 5 (December) (2019) 101–112.
[24] E. Bwambale, P. Home, J. Raude, J. Wanyama, Development of a water allocation model for equitable water distribution at Doho Rice Irrigation Scheme, Uganda, Hydrology 7 (4) (2019) 62, https://doi.org/10.11648/j.hyd.20190704.12.
[25] M. Rodell, et al., The global land data assimilation system, Bull. Am. Meteorol. Soc. 85 (2004) 381–394.
[26] M. Cai, S. Yang, C. Zhao, H. Zeng, Q. Zhou, Estimation of daily average temperature using multisource spatial data in data sparse regions of Central Asia, J. Appl. Remote Sens. 7 (2013), 073478.
[27] J.K. Kiptala, Y. Mohamed, M.L. Mul, P. Zaag, Mapping evapotranspiration trends using MODIS and SEBAL model in a data scarce and heterogeneous landscape in Eastern Africa, Water Resour. Res. 49 (2013) 8495–8510.
[28] T. He, et al., Remote Sensing of Environment Evaluating land surface albedo estimation from Landsat MSS, TM, ETM +, and OLI data based on the uni fi ed direct estimation approach, Remote Sens. Environ. 204 (July 2016) (2018) 181–196, https://doi.org/10.1016/j.rse.2017.10.031.
[29] A.N. Bruno Sánchez, Visualizing NDVI for Agriculture | by Mapbox | Maps for Developers, 2014.
[30] A. Sekertekin, S. Bonafoni, Land surface temperature retrieval from Landsat 5, 7, and 8 over rural areas: assessment of different retrieval algorithms and emissivity models and toolbox implementation, Remote Sens 12 (2) (2020), https://doi.org/10.3390/rs12020294.
[31] L. Jia, G. Xi, S. Liu, C. Huang, Y. Yan, G. Liu, Regional estimation of daily to annual regional evapotranspiration with MODIS data in the Yellow River Delta wetland, Hydrol. Earth Syst. Sci. 13 (10) (2009) 1775–1787, https://doi.org/10.5194/hess-13-1775-2009.
[32] D.T. Rwasoka, W. Gumindoga, J. Gwenzi, Estimation of actual evapotranspiration using the Surface Energy Balance System (SEBS) algorithm in the Upper Manyame catchment in Zimbabwe, Phys. Chem. Earth, Parts A/B/C 36 (14–15) (2011) 736–746, https://doi.org/10.1016/j.pce.2011.07.035.
[33] E. Costa-Filho, J.L. Chávez, H. Zhang, A.A. Andales, An optimized surface aerodynamic temperature approach to estimate maize sensible heat flux and evapotranspiration, Agric. For. Meteorol. 311 (May 2021), https://doi.org/10.1016/j.agrformet.2021.108683.
[34] W. Brutsaert, H. Stricker, An advection-aridity approach to estimate actual regional evapotranspiration, Water Resour. Res. 15 (2) (1979) 443–450, https://doi.org/10.1029/WR015i002p00443.
[35] F. Akhtar, U. Awan, B. Tischbein, U. Liaqat, Assessment of irrigation performance in large river basins under data scarce environment—a case of Kabul River Basin, Afghanistan, Remote Sens. 10 (6) (2018) 972, https://doi.org/10.3390/rs10060972.
[36] M. Cooper, "Advanced bash-scripting guide an in-depth exploration of the art of shell scripting table of contents," *Okt 2005 Abrufbar uber httpwww tldp orgLDPabsabsguide pdf Zugriff 1112 2005*, vol. 2274, no. November 2008, pp. 2267–2274, 2010, doi: 10.1002/hyp.
[37] J.L. Monteith. and M.H. Unsworth, *Principles of Environmental Physics*, 2nd edn. Woburn, Massachusetts., 1990.
[38] H.L. Penman, Natural evaporation from open water, bare soil and grass, Proc. Roy. Soc. London A 193 (1948) 120–145.
[39] P.E. Rijtema, An analysis of actual evapotranspiration, Soil Sci. Soc. Am. J. 29 (6) (1965) vi, https://doi.org/10.2136/sssaj1965.03615995002900060007x. –vi.
[40] C. Priestley, R. Taylor, On the assessment of surface heat flux and evaporation using large-scale parameters, Mon. Weather Rev. 100 (1972) 81–92.
[41] H. Penman, Evaporation: an introductory survey, Netherlands J. Agric. Sci. 4 (1956) 9–29.
[42] M.E. Jensen and R.G. Allen, *Evaporation, evapotranspiration, and irrigation water requirements*, vol. 2016, no. 70. 2016.
[43] R. Allen, L.S. Pereira, D. Raes, M. Smith, Crop Evapotranspiration—Guidelines for Computing Crop Water Requirements, 56, FAO, 1998.
[44] M. Svendsen, L.E. Small, Farmer's perspective on irrigation performance, Irrig. Drain. Syst. 4 (1990) 385–402.
[45] M.G. Bos, D.H. Murray-Rust, D.J. Merrey, H.G. Johnson, W.B. Snellen, Methodologies for assessing performance of irrigation and drainage management, Irrig. Drain. Syst. 7 (4) (1993) 231–261, https://doi.org/10.1007/BF00881553.
[46] U.K. Awan, B. Tischbein, C. Conrad, C. Martius, M. Hafeez, Remote sensing and hydrological measurements for irrigation performance assessments in a water user association in the Lower Amu Darya River Basin, Water Resour. Manag. 25 (2011) 2467–2485.
[47] C.J. Perry, Quantification and measurement of a minimum set of indicators of the performance of irrigation systems, Int. Irrig. Manag. Inst. Colombo, Sri Lanka (1996).
[48] K.M.P.S. Bandara, "Assessing irrigation performance by using remote sensing," 2006.
[49] J. Asaana and A. Sadick, "Assessment of irrigation performance using remote sensing technique at tono irrigation area in the upper east region of Ghana," vol. 1, no. 4, pp. 79–91, 2016.